

Structured jets in TeV BL Lac objects and radio galaxies

Gabriele Ghisellini¹, Fabrizio Tavecchio¹ and Marco Chiaberge²

¹ Osservatorio Astronomico di Brera, via Bianchi 46, I-23807 Merate, Italy;

² IRA/CNR, via Gobetti 101, I-40129, Bologna, Italy

Received 2004

Abstract. TeV BL Lacertae objects require extreme relativistic bulk motion in the gamma-ray emission region, but at the VLBI scale their radio knots hardly move. The same sources show evidences, in radio, of a structure made of a fast spine plus a slow layer. We propose that this structure exists even at the gamma-ray scale. One component sees the (beamed) radiation produced by the other, and this enhances the inverse Compton emission of both components. In addition, this allows the magnetic field to be nearly in equipartition with the emitting particles. The inverse Compton emission of the spine is anisotropic in its frame, possibly producing the deceleration of the spine by the Compton rocket effect. In this scenario, also the slow layer is a relatively strong high energy emitter, and thus radio galaxies become potentially detectable by GLAST.

Key words. Galaxies: jets — BL Lacertae objects: general — Radio continuum: galaxies — Radiation mechanisms: non-thermal — Gamma-rays: theory

1. Introduction

There is growing evidence from VLBI studies that pc scale jets in strong TeV BL Lacs move slowly (Edwards & Piner 2002; Piner & Edwards 2004; Giroletti et al., 2004). On the contrary, the bright and rapidly variable TeV emission implies that at the jet scales where this emission originates, the jet should be highly relativistic. This is necessary in order to avoid the absorption of TeV photons by the IR radiation produced cospatially to the TeV emission (see e.g. Dondi & Ghisellini 1995). Furthermore, fitting the SED of TeV sources with a simple, one-zone homogeneous synchrotron self-Compton (SSC) model allows to univocally determine the physical parameters of the emitting region (Tavecchio, Maraschi & Ghisellini 1998), and in fact all authors applying SSC models derive similar values of the Doppler factor, in the range 10–20, when the TeV spectrum is not de-reddened by the absorption of TeV photons by the IR background (Tavecchio et al. 2001, Kino, Takahara & Kusunose 2002; Ghisellini, Celotti & Costamante 2002; Katarzynski, Sol & Kus 2003), and larger (up to 50) when the TeV spectrum is dereddened (Krawczynski, Coppi & Aharonian 2002; Konopelko et al. 2003). It is therefore clear that the jet must suffer a severe deceleration from the γ -ray emitting zone (~ 0.1 pc from the jet apex) to the VLBI (~ 1 pc) scale.

Prompted by these observational evidences, Georganopoulos & Kazanas (2003, hereafter GK03) have proposed that if the entire jet is fastly decelerating in the γ -ray zone, then the base of the jet, still moving fast, will see the radiation produced

at the end of the deceleration zone relativistically boosted. These “extra” radiation will favor the inverse Compton emission, allowing to derive less extreme values of the physical parameters with respect to a pure one-zone SSC model. Our paper is german to the one of GK03, but we study the alternative hypothesis that the jet is structured not in the radial direction, but in the transverse one, being composed by a slow layer and a fast spine.

We are motivated by the recent observational evidence coming from detailed VLBI (including space VSOP observations) radio maps, showing, in Mkn 501, a *limb brightening* morphology, interpreted as evidence of a slower external flow surrounding a faster spine (Giroletti et al. 2004). Similar results have been obtained for a few radio galaxies (Swain et al. 1998; Owen et al 1989; Giovannini et al. 1999). Apart from observational evidence, a spine–layer configuration for the jet has been proposed in the past on the basis of theoretical arguments (e.g., Henri & Pelletier 1991). In addition, the existence of a velocity structure has also been suggested to explain some observed properties of radio galaxies, such as their magnetic field configuration (Komissarov 1990; Laing 1993), and to overcome problems unifying radio galaxies with BL Lac objects (Chiaberge et al. 2000).

We also hope that this assumption helps to find a possible reason for the deceleration of (at least a part of) the jet, which was *postulated* by GK03. A slow layer could in fact be the result of the interaction of the “walls” of the jet with the ambient medium, or simply be the result of a jet acceleration which is

a function of the angular distance from the jet axis,¹ producing a velocity structure. Kelvin–Helmholtz instabilities (for review see Ferrari 1998), while important for the formation of the layer, may not decelerate (and destroy) the entire jet (e.g. Bodo et al. 2003), especially if the jet itself is not continuous, but “intermittent”, as in the internal shock scenario (Ghisellini 1999, Spada et al. 2001, Guetta et al. 2004). Note in fact that the dynamical timescale involved in internal shocks is approximately the light crossing time across the source, while instabilities can grow with the sound speed.

As in the decelerating scenario proposed by GK03, there will be a strong radiative interplay and feedback between the layer and the spine: both parts see extra seed photons coming from the other part, and this will enhance the inverse Compton emission of *both* components. This may help explaining why also radiogalaxies can be relatively strong γ -ray emitters, as suggested by the Comptel and EGRET (onboard the Compton Gamma Ray Observatory) detection of Centaurus A (Steinle et al. 1998 and references therein), the recent identifications of NGC 6251 with an EGRET source (Mukherjee et al. 2002), and the possible detection of M87 at TeV energies (Aharonian et al. 2003). This emission, coming from the inner part of the relativistic jet of radiogalaxies, should be characterized by a pronounced variability: this could help to distinguish it from the high energy radiation coming from the more extended (kpc) parts of the jet, as suggested by Stawarz et al. (2004).

In Section 2 we present the basic assumptions of the model, which we apply, in Section 3, to Mkn 421, Mkn 501, Cen A and also to NGC 6251, assumed to be “twined” with the classic BL Lac PKS 0735+178. Even if these “fits” are not unique solutions (given the large number of free parameters), they illustrate the radiative feedback between the spine and the layer. In Section 4 we discuss what we think is a major outcome of the scenario we are proposing, namely the possibility that the spine can recoil under the effect of its own inverse Compton emission (Compton rocket effect). Since it is natural, in our model, that also the inverse Compton emission of the layer is enhanced, we stress in Section 5 that radiogalaxies, not only blazars, can be bright γ -ray emitters, and we present a preliminary list of possible candidates for detection by GLAST. In Section 6 we discuss our results and draw our conclusions.

2. The model

We assume that the layer can be approximated as an hollow cylinder, with external radius R_2 , internal radius R and width $\Delta R_l''$, as measured in the comoving frame of the layer². The comoving volume of the layer is then $V_l'' = \pi(R_2^2 - R^2)\Delta R_l''$. Also for the spine we assume a cylindrical geometry, with the same R and a width $\Delta R_s'$, as measured in the comoving frame of the spine. The active volume of the spine is then $V_s' = \pi R^2 \Delta R_s'$. Fig. 1 illustrates the assumed geometry. The

¹ Note that the possibility of structured jets has been proposed and somewhat explored also for Gamma–Ray Bursts, see Rossi, Lazzati & Rees 2001; Zhang & Meszaros 2002.

² Primed quantities are in the rest frame of the spine, double primed quantities are in the frame of the layer.

Lorentz factors of the spine and of the layer are Γ_s and Γ_l , respectively, with $c\beta_s$ and $c\beta_l$ the corresponding velocities. Since the spine and the layer move with different Lorentz factors, the radiation emitted by the spine (layer) is seen boosted by the layer (spine). With respect to a comoving observer at the same distance from the spine (layer), the radiation energy density is enhanced by a factor $\sim (\Gamma')^2$, with Γ' given by

$$\Gamma' = \Gamma_s \Gamma_l (1 - \beta_s \beta_l) \quad (1)$$

Both structures emit by the synchrotron and the inverse Compton processes. The energy distribution of the emitting electrons, $N(\gamma)$, is assumed to extend down to γ_{\min} , and is assumed to have the shape:

$$N(\gamma) = K \gamma^{-n_1} \left[1 + \left(\frac{\gamma}{\gamma_b} \right)^{n_1 - n_2} \right] e^{-\frac{\gamma}{\gamma_{\text{cut}}}}; \quad \gamma > \gamma_{\min}$$

$$N(\gamma) = 0, \quad \gamma \leq \gamma_{\min} \quad (2)$$

The normalization (i.e. K) of this distribution is found by imposing that $N(\gamma)$ produces a given intrinsic synchrotron luminosity, which is an input parameter of the model.

The seed photons relevant for the scattering process are produced not only by the spine (layer) electrons, but also by the layer (spine) ones. There is a strong *feedback* between the two components, which determines the amount of inverse Compton radiation emitted by both structures (if this process is important with respect to the synchrotron one). As a general rule, this feedback increases the inverse Compton flux, since both the spine and the layer see an enhanced radiation energy density. Since the ratio between the radiation and the magnetic energy densities U_B/U_{rad} measures (even if it is not equal, for scatterings in the Klein Nishina regime) the ratio between the inverse Compton and the synchrotron luminosities, an enhanced U_{rad} in turn implies a larger magnetic field. Therefore both the synchrotron and the inverse Compton luminosities can be produced by a reduced number of relativistic electrons (radiatively cooling in a shorter time with respect to the case of no feedback). This fact bears important consequences for the energetics and the dynamics of the jet, and will be discussed in Section 4.

The length of the layer, as observed in a frame comoving with the spine, is $R_l' = R_l''/\Gamma'$. Analogously, the length of the spine, as observed in the frame comoving with the layer, is $R_s'' = R_s'/\Gamma'$. In the following, we will always assume that the layer is longer than the spine, even in the frame of the spine. To calculate the radiation energy density of one component as observed by the other, we will assume the following:

- Let us call $\bar{R} \equiv (R_2 + R)/2$. In the comoving frame of the layer, the radiation energy density in the entire cylinder is assumed to be $U_l'' = L_l''/(\pi \bar{R}^2 c)$. In the frame of the spine, this radiation energy density is assumed to be boosted by a factor $(\Gamma')^2$, i.e. $U_l' = (\Gamma')^2 U_l''$.
- In the comoving frame of the spine, the radiation energy density within the spine is assumed to be $U_s' = L_s'/(\pi R^2 c)$. In the frame of the layer, this radiation energy density is observed to be boosted by $(\Gamma')^2$, but also diluted (since the layer is larger than the spine) by the factor $\Delta R_s''/\Delta R_l'' = (\Delta R_s'/\Gamma')/\Delta R_l''$.

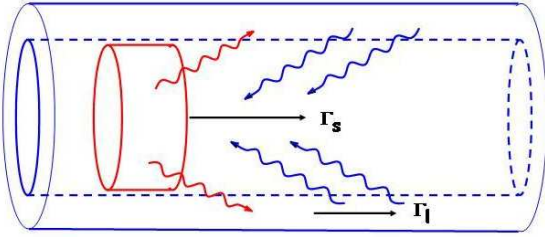


Fig. 1. Cartoon illustrating the layer+spine system.

While the synchrotron and the SSC emission in the comoving frame is assumed to be isotropic, the inverse Compton process between electrons of the layer (spine) and seed photons produced by the spine (layer) is highly anisotropic. Dermer (1995) found the pattern of the emitted radiation from a moving blob immersed in a bath of seed photons (e.g. corresponding to the radiation produced by the broad line region of a powerful blazar), and pointed out the fact that in this case the external Compton radiation is more beamed than the synchrotron and SSC emission.

In our case the component contributing to the “external” radiation is not at rest with the distant observer, but moves. To find out the pattern of the emitted radiation it is convenient to move to the comoving frame of the emitter of the seed photons. Consider then the seed photons produced by the layer, and an observer comoving with the layer. In this frame, the spine is moving with Γ' , and the photon frequencies produced by the spine are blueshifted by the Doppler factor ³ $\delta_{s,l}$. Going to the frame of the distant observer, these photons are further blueshifted by δ_l . But the distant observer will see the same photons blueshifted by δ_s . This implies

$$\delta_{s,l} \delta_l = \delta_s \quad (3)$$

We can repeat the same argument for photons produced by the layer. We then have

$$\delta_{s,l} = \frac{\delta_s}{\delta_l} = \frac{1}{\delta_{l,s}} \quad (4)$$

This nice argument is due to GK03.

In the frame of the layer the external Compton radiation produced by the spine follows a pattern $\propto \delta_{s,l}^{4+2\alpha}$ (Dermer 1995), where α is the spectral index of the emission [$F(\nu) \propto \nu^{-\alpha}$], while the synchrotron and SSC emission follows the usual pattern $\propto \delta_{s,l}^{3+\alpha}$. If $I'(\nu')$ is the monochromatic intrinsic intensity produced by the spine, we have

$$I(\nu) = I'(\nu') \delta_{s,l}^{4+2\alpha} \delta_l^{3+\alpha} = I'(\nu') \delta_s^{3+\alpha} \left(\frac{\delta_s}{\delta_l} \right)^{1+\alpha} \quad (\text{EC})$$

$$I(\nu) = I'(\nu') \delta_s^{3+\alpha} \quad (\text{S, SSC}) \quad (5)$$

Here S stands for synchrotron, EC for “external Compton” (scattering of the seed photons coming from the layer). In the

³ $\delta = \Gamma^{-1}(1 - \beta \cos \theta)^{-1}$, where θ is the viewing angle. Note that Γ and θ are different in different frames. $\delta_{s,l}$ is defined as the beaming factor of the radiation produced in the spine as observed in the layer.

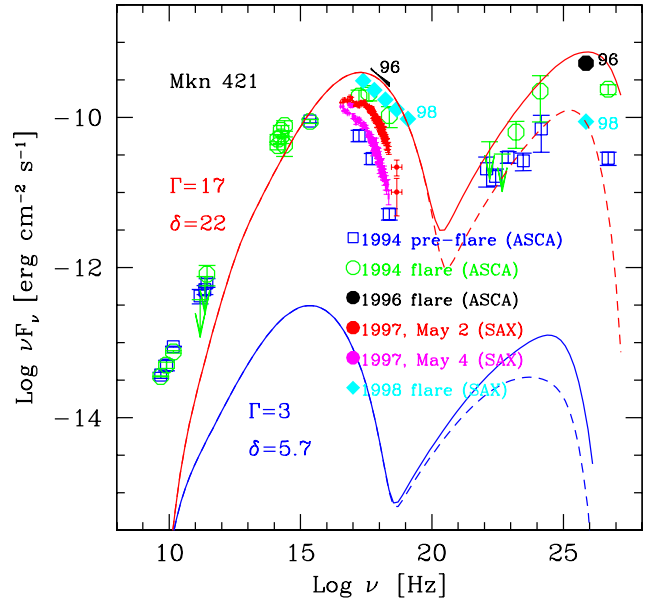


Fig. 2. Example of the SED produced by the spine–layer system, using the parameters listed in Tab. 1. The contribution of the spine and the layer in each panel are labelled. Dashed lines correspond to the emission of the spine (layer) without taking into account the seed photons coming from the layer (spine). For the data points see Costamante & Ghisellini (2002) and references therein.

case of radiation produced by the layer, the transformation is the same, with δ_s and δ_l interchanged.

Free parameters — For each component the input parameters are: $\Delta R'$, B , L'_{inj} , Γ , γ_{min} , γ_b , γ_{cut} , n_1, n_2 . Parameters equal for both components are R and the viewing angle θ . The outer radius of the layer R_2 must also be specified, but we will always use $R_2 = 1.2R$. For $n_2 > 3$, γ_{cut} becomes unimportant and we have a total of 18 parameters. While they appear (and are) many, we stress that the aim of this paper is to discuss the main effects of having the layer+spine structure, and not (yet) the exact determination of the physical quantities inside the source. In other words, we have to model *two* structures by observing the radiation coming from only one of them, and this will leave some ambiguity, unless we find information about the layer (spine) even if we are observing the spine (layer) emission ⁴.

3. Results

We have applied the model to the two best studied TeV BL Lacs: Mkn 501 and Mkn 421, and to the radiogalaxy Cen A. In addition, we have tried to see if our spine+layer structure can explain *at the same time* the emission from a “classical” BL Lac

⁴ One possibility could be the observation, in radiogalaxies, of emission lines resulting from photoionization due to the spine radiation (Morganti et al. 1992), or the knowledge of the total power carried by the entire jet through estimates of the total energy and age of the extended radio structure (as done by Rawlings & Saunders 1991).

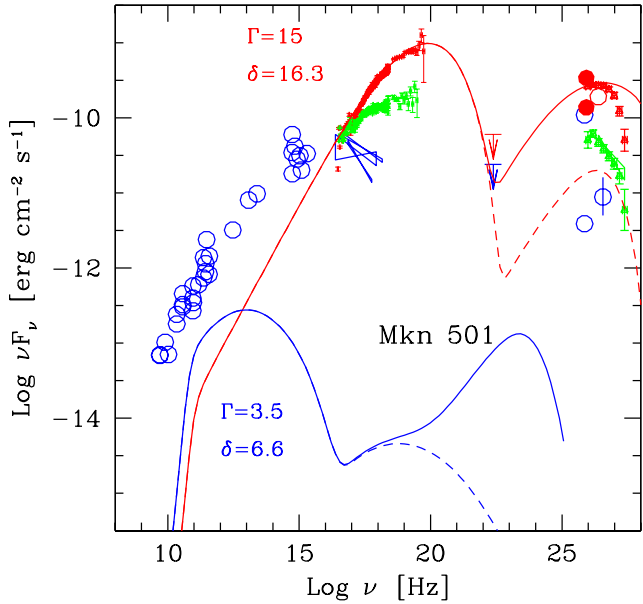


Fig. 3. Example of the SED produced by the spine–layer system, using the parameters listed in Tab. 1. The contribution of the spine and the layer in each panel are labelled. Dashed lines correspond to the emission of the spine (layer) without taking into account the seed photons coming from the layer (spine). Data from Pian et al. (1998) and Djannati-Atai et al. (1999).

object, PKS 0735+178, and the radiation observed for the radiogalaxy NGC 6251, which has been recently associated with an EGRET source. In other words, we check if these two apparently very different objects, at very different distances (but both emitting high energy γ -rays), can be considered as “twins”. Note that the radio luminosity $L_{1.4}$ at 1.4 GHz of the two objects, indicative of the extended (and unbeamed) radio power, is almost equal (for PKS 0735+178: $L_{1.4} = 9 \times 10^{31}$ erg s^{-1} Hz^{-1} , Cassaro et al. 1999; for NGC 6251: $L_{1.4} = 3 \times 10^{31}$ erg s^{-1} Hz^{-1} , Laing, Riley & Longair, 1983, extrapolating from 178 MHz with a radio spectral index $\alpha = 0.7$). In this case the differences in the observed nuclear SED are due entirely to a different viewing angle θ , enhancing the spine or the layer emission for small and large θ , respectively.

We stress however that our aim is not to precisely fit the SED of these sources, since our results are not unique. For instance, the parameters for the layer of Mkn 421 and Mkn 501 have been chosen with the aim to increase the allowed value of the magnetic field of the corresponding spines. In other words, we applied a theoretical prejudice, aiming to bring these sources closer to equipartition than a simple one zone SSC model allows to. Other poorly constrained parameters are the width of the layer and its bulk Lorentz factor. For the former we simply require $\Delta R'' > R$, for the latter we have the requirement that the counterjet is, in these sources, invisible up to the few tens of m.a.s. scale, leading to a limit of $\Gamma_l > 2–3$.

Concerning the “twin” exercise we have much less freedom, of course, but it is the choice of these two sources which

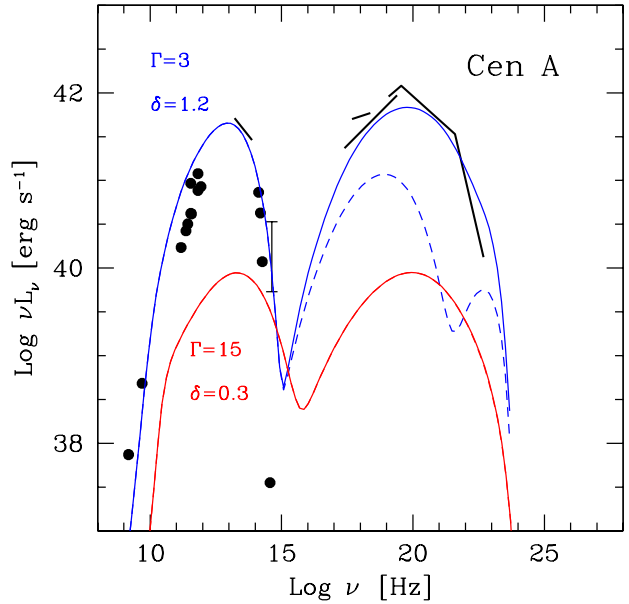


Fig. 4. The SED of Cen A is modelled by the spine–layer system, using the parameters listed in Tab. 1. The contribution of the spine and the layer in each panel are labelled. Dashed lines correspond to the emission of the spine (layer) without taking into account the seed photons coming from the layer (spine). For the spine the dashed and continuous lines overlap. Data from Chiaberge, Capetti & Celotti (2001) and references therein.

is somewhat arbitrary, even if both are γ -ray emitters and presumably both belong to the FR I class of radiogalaxies.

In conclusion, our aim is to demonstrate that our model can consistently work both for radiogalaxies and BL Lacs, and this allows to draw some general conclusions about their jets and the importance of the inverse Compton emission. The input parameters used for the models shown in Figs. 2–4 are all listed in Table 1, while Table 2 reports the values of the kinetic powers carried by the spine and the layer, the average (and the average of the square) of the random Lorentz factor of the emitting electrons, and the relative bulk Lorentz factor Γ' . The kinetic powers are defined as

$$L_i = \pi R^2 \Gamma^2 \beta c U_i \quad (6)$$

where the energy density U_i refer to: electrons ($U_e = \int N(\gamma) \gamma m_e c^2 d\gamma$); magnetic field ($U_B = B^2/(8\pi)$); protons (U_p), assuming one cold proton per electron; total radiation (U_{rad}) and synchrotron radiation (U_{syn}).

In all cases shown in Figg. 2–4, continuous lines show the results of the models including the spine–layer radiative feedback, while the dashed lines are the results of the same models neglecting the feedback.

– **Mkn 501:** Fig. 2 shows the “fits” to the SED of Mkn 501 in its flaring state of April 1997 (Pian et al. 1998). Note the rather moderate bulk Lorentz factor used for the spine ($\Gamma_s = 15$), which has the same value of the one used by

GK03. The rather large value of the magnetic field ensures nearly equipartition between magnetic and particle energy.

- **Mkn 421:** Fig. 3 shows our model compared with different simultaneous SED of this source, and aiming to “fit” the highest state. The bulk Lorentz factor of the spine is $\Gamma_s = 17$, which at a viewing angle $\theta = 2.5^\circ$ leads to a beaming factor $\delta = 22$. The remarkable difference with respect to a simple one zone SSC models is the much larger value of the magnetic field: 1 Gauss compared with $B \sim 0.02\text{--}0.1$ Gauss (see the references quoted in the Introduction) This bring the magnetic energy in equipartition with particle energy, dominated in this case by the energetic electrons, which have a very large average random Lorentz factor ($\langle \gamma \rangle = 1900$, and therefore $\langle \gamma \rangle m_e \sim m_p$). This is due both to the relatively large value of γ_{\min} and the flat electron slope at low energies, in turn required in order not to overproduce the IR emission.
- **Cen A:** As can be seen in Fig. 4, the synchrotron emission in this object is particularly narrow, with a peak in the far IR. This indicates a corresponding narrow energy distribution of the emitting electrons. We have assumed a viewing angle of $\theta = 40^\circ$, corresponding to a modest beaming of the layer emission ($\delta = 1.2$), and a severe de-beaming of the spine radiation ($\delta = 0.28$). Comparing the jet powers of this source with Mkn 421 or Mkn 501, we find that the jet of Cen A is more powerful, with most of the power carried by the spine.
- **PKS 0735+178:** This “classic” BL Lac has been detected by EGRET (Hartman et al. 1999), and shows a relatively flat X-ray spectrum, signature of the fact that at these energies the inverse Compton emission is already dominating. The synchrotron peak frequency lies in the IR–optical and possibly “moves” within these bands. The data shown in Fig. 4 are not simultaneous, and therefore give a rough idea of the entire SED. Nevertheless it is clear that this source belongs to the LBL (Low energy peak BL Lac, see Giommi & Padovani 1995) category. There is only a lower limit for its redshift, ($z > 0.424$); for the modeling we assume $z = 0.424$. The implied energetics are two orders of magnitude larger than for the previous sources, if a similar value of the Doppler beaming factor is appropriate. Accordingly, we have assumed a larger intrinsic power, and a larger value of the magnetic field. This brings the magnetic energy closer to equipartition (with respect to a pure SSC model) with the energy contained in the relativistic electrons.
- **NGC 6251:** The layer assumed to be in the jet of PKS 0735+178, if observed at 20° , becomes the dominant contributor to the SED and give rise to the spectrum of the nearby radiogalaxy NGC 6251 ($z = 0.0249$), as illustrated in the bottom panel of Fig. 4. Note that also in this case the data points are not simultaneous, and can give only a rough idea of the overall (nuclear) SED of this object. Therefore the slight overproduction of X-rays predicted by the model is not (yet) necessarily a failure of the model. Note also that when the layer is not illuminated by the spine (and this can happen, since the spine can be constituted by discontinuous blobs), then the predicted emission corresponds to the

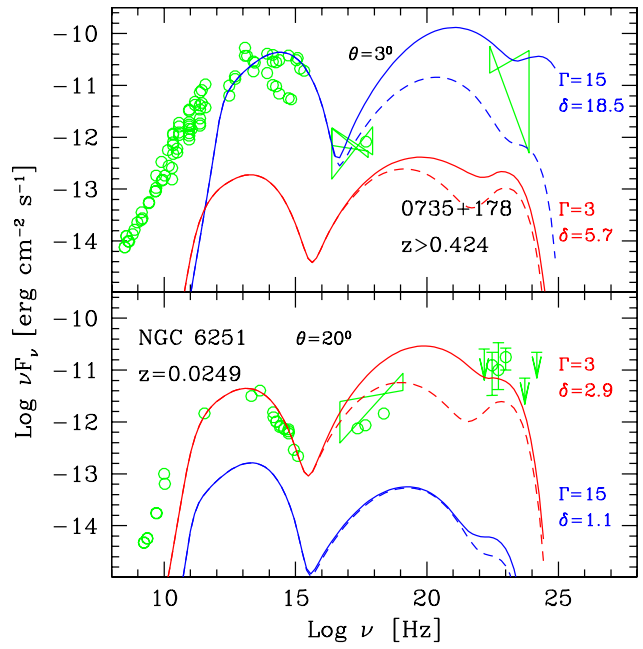


Fig. 5. Example of the SED produced by the spine–layer system, using the parameters listed in Tab. 1. The viewing angle is $\theta = 2^\circ$ for the example shown in the upper panel, and $\theta = 22^\circ$ for the bottom panel. The model is compared with the data of the BL Lac PKS 0735+178 (top) and the FR 1 radiogalaxy NGC 6251 (bottom). The contribution of the spine and the layer in each panel are labelled. Dashed lines correspond to the emission of the spine (layer) without taking into account the seed photons coming from the layer (spine). Data from Ghisellini et al. (1998) and Chiaberge et al. (2003) and references therein.

dashed line, which is closer to the X-ray data, but under-predicts the γ -ray flux. This may originate two different states of the source, and EGRET could detect the object only when the layer was illuminated by the spine.

From the exercise of “fitting” the SED of the previous few BL Lacs (and a radiogalaxy), we can draw the following general conclusions:

- The feedback between the layer and the spine enhances the inverse Compton emission in both components. In the shown examples, the enhancement is around one order of magnitude, or even greater.
- The magnetic field is larger, in this spine/layer scenario, and is consistent with being in equipartition with the relativistic electrons.
- The larger magnetic field implies that, to produce the same amount of synchrotron radiation, less electrons are needed. If there is one proton per electrons, we need also less protons. This implies a decrease in the total jet kinetic power (with respect to a pure SSC model).
- The examples shown here assume that the spine is active only when inside the layer. But other possibilities exist: for instance, the layer could be particularly narrow (i.e. small ΔR_l), and allow the spine to survive the passage through

	R cm	$\Delta R'$ cm	L'_{syn} erg s $^{-1}$	B G	γ_{min}	γ_{b}	γ_{cut}	n_1	n_2	Γ	θ
Mkn 421 (spine)	3e15	1e15	3.0e40	1.1	2e2	3e4	1e6	1.5	3.5	17	2.5
Mkn 421 (layer)	3e15	3e16	5.0e39	0.5	50	1e4	3e5	1.5	3.5	3	2.5
Mkn 501 (spine)	3e15	1e15	2.5e41	1.3	1	3e5	1e7	1.7	2.6	15	3.5
Mkn 501 (layer)	3e15	3e16	3.0e39	1	1	3e2	3e4	1.5	3.5	3.5	3.5
Cen A (spine)	1e16	1e15	8.0e42	4	50	3e3	3e4	1.5	4	15	40
Cen A (layer)	1e16	1e17	1.0e42	2	1e2	4e3	4e3	1.0	4	3	40
PKS 0735+178/NGC 6251 (spine)	5e15	5e14	1.0e42	5	50	2e3	6e3	1.5	3	15	3/20
PKS 0735+178/NGC 6251 (layer)	5e15	2.5e16	5.0e41	1.8	1e2	2e3	1e4	1.6	4.5	3	3/20

Table 1. Input parameters of the models for the layer and the spine shown in Figg. 2–5. Note that we have assumed that the viewing angles for PKS 0735+178 and for NCG 62151 are 3° and 20° respectively.

	L_e erg s $^{-1}$	L_p erg s $^{-1}$	L_B erg s $^{-1}$	L_r erg s $^{-1}$	L_s erg s $^{-1}$	$\langle \gamma \rangle$	$\langle \gamma^2 \rangle$	Γ'	δ
Mkn 421 (spine)	1.0e43	9.7e42	1.2e43	1.3e43	8.9e42	1.9e3	3.1e7	3.0	21.9
Mkn 421 (layer)	2.5e40	8.5e40	3.2e40	1.2e41	5.6e39	5.4e2	2.8e6	3.0	5.7
Mkn 501 (spine)	3.7e42	6.7e43	1.3e43	6.1e43	5.8e43	102	2.1e7	2.3	16.3
Mkn 501 (layer)	1.3e41	1.7e43	1.7e41	5.9e40	3.9e39	14	2.9e3	2.3	6.6
Cen A (spine)	2.7e45	1.9e46	1.3e45	4.6e45	1.8e45	2.6e2	2.5e5	2.7	0.28
Cen A (layer)	7.7e41	4.1e42	2.7e41	5.1e43	9.6e41	3.5e2	2.2e5	2.7	1.2
PKS 0735+178/NGC 6251 (spine)	8.0e44	7.4e45	5.3e44	4.0e44	2.2e44	198	1e5	2.7	18.6
PKS 0735+178/NGC 6251 (layer)	2.3e42	1.6e43	5.4e41	3.9e43	9.4e41	271	1.4e5	2.7	2.9

Table 2. Derived jet powers and parameters of the models for the layer and the spine shown in Figg. 2 – 5.

itself (i.e. the electrons may not cool completely). In such a case, the spine will continue to emit the same amount of synchrotron radiation (if the particle distribution does not change), while the amount of high energy emission will drastically decrease. This might explain the “orphan TeV flares” (i.e. flares in the TeV band not accompanied by simultaneous flares in the X-ray band) observed in simultaneous RXTE/TeV observations (Krawczynski et al. 2004).

- To be effective, the layer must of course be located in the same region of the jet where the spine undergoes dissipation and emits. In other words, it must be compact, even if its width can be larger (factor ~ 10) than the spine width (i.e. $\Delta R_l \sim 10 \Delta R'_s$). This implies variability of the layer. Even if its particle distribution is steady, in fact, its high energy emission will change as the spine is illuminating it or not (e.g. compare the continuous and dashed lines for the layer in Figg. 2–4).

4. Energetics and dynamics

As can be seen in Table 2, the power spent to emit the inverse Compton radiation is significant, if compared with the total bulk kinetic power contained in the relativistic electrons and protons. As described above, this luminosity is emitted anisotropically in the comoving frame of the spine, hence the spine must recoil. Since this *Compton rocket* effect is a potentially important deceleration mechanism, we discuss it here in more detail.

The most convenient frame where to study the dynamics of the spine is the frame comoving with the layer. In this frame the synchrotron radiation produced by the layer is isotropic, with energy density U'_{syn} . To avoid an excess of symbolism, from

now on (unless otherwise noted) the unprimed quantities are measured in the frame of the layer, and the primed quantities are evaluated in the frame of the spine. For the same reason we let the random Lorentz factor unprimed, with the notion that these Lorentz factors are measured in the frame of the spine, where they are assumed to be isotropically distributed.

The total Lorentz factor ($\tilde{\gamma}$) of the electrons is the superposition of the relative bulk (Γ) and random (γ) Lorentz factors. Assume that the random velocity forms an angle θ' with respect to the jet axis, in the spine frame. From Rybicki & Lightman (1979) we have:

$$\begin{aligned} \beta_x &= \frac{\beta' \cos \theta' + \beta_{\text{bulk}}}{1 + \beta_{\text{bulk}} \beta' \cos \theta'} \\ \beta_y &= \frac{\beta' \sin \theta'}{\Gamma_{\text{bulk}} (1 + \beta_{\text{bulk}} \beta' \cos \theta')} \end{aligned} \quad (7)$$

The total $\tilde{\gamma}^2$ is

$$\begin{aligned} \tilde{\gamma}^2 &= [1 - \beta_x^2 - \beta_y^2]^{-1} \\ &= (1 + \beta_{\text{bulk}} \beta' \cos \theta')^2 \gamma^2 \Gamma^2 \end{aligned} \quad (8)$$

If the particle distribution is isotropic in the spine frame, the average over angles gives

$$\begin{aligned} \langle \tilde{\gamma}^2 \rangle &= \frac{\int 2\pi \sin \theta' \tilde{\gamma}^2(\theta') d\theta'}{4\pi} \\ &= \frac{\gamma^2 \Gamma^2}{2} \int_{-1}^1 (1 + \beta_{\text{bulk}} \beta' \mu')^2 d\mu' \\ &= \left[1 + \frac{(\beta_{\text{bulk}} \beta')^2}{3} \right] \gamma^2 \Gamma^2 \end{aligned} \quad (9)$$

which gives the factor $(4/3)$ for ultrarelativistic speeds.

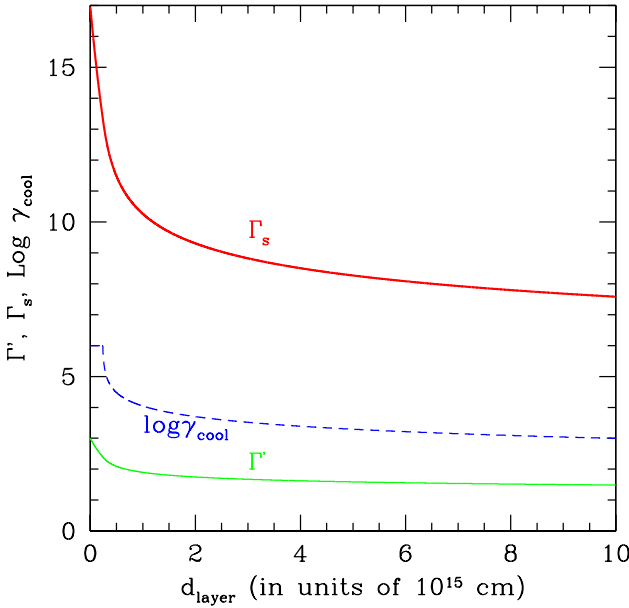


Fig. 6. The bulk Lorentz factor as a function of distance as measured in the frame of the layer and in the earth frame. Also shown, as labelled, is the logarithm of γ_{cool} . We have adopted the same parameters as the ones used for Mkn 421 and reported in Table 1.

The loss of energy of the jet is proportional to $\langle \tilde{\gamma}^2 \rangle$, and the loss of momentum is the component along the jet axis of the loss of energy. In other words, we have to calculate the quantity

$$\langle \tilde{\gamma}^2 \rangle_z = \frac{\int 2\pi\mu' \tilde{\gamma}^2(\theta') d\mu'}{4\pi} = \frac{2}{3} \beta_{\text{bulk}} \beta' \gamma^2 \Gamma^2 \quad (10)$$

Now assume that the spine carries N_p protons (total number) and N_e leptons. The loss of momentum of the jet is described by:

$$\begin{aligned} \frac{d\Gamma}{dt} &= \frac{4}{3} \frac{\sigma_T c N_e U_{\text{syn}} \langle \tilde{\gamma}^2 \rangle_z}{N_p m_p c^2 + N_e \langle \gamma \rangle m_e c^2} \\ &= \frac{8}{9} \frac{\sigma_T c N_e U_{\text{syn}} \langle \gamma^2 \rangle \Gamma^2}{N_p m_p c^2 + N_e \langle \gamma \rangle m_e c^2} \end{aligned} \quad (11)$$

We remind that the bulk Lorentz in Eq. (11) is the relative Lorentz factor (which is the Lorentz factor of the spine as measured in the layer). A detailed analysis of this Compton rocket effect in AGN jets has been presented by Sikora et al. (1996). They derive the equations regulating the drag effect and apply the results to the case of jets in radio-loud quasars with strong emission lines. Eq. (11), although obtained in a rather simplified way, coincides with the results of Sikora et al. (for the specific case of isotropic radiation field).

To find the value of Γ_s as measured by an observer at earth, one must invert Eq. 1. It must be noted that, in general, $\langle \gamma \rangle$ and $\langle \gamma^2 \rangle$ are not constant, but can change due to e.g. radiative cooling. We have integrated Eq. 11 assuming:

- The particle distribution remains unaltered for a time equal to the light crossing time of the spine (i.e. $\Delta R_s/c$) as measured in the frame of the layer. This corresponds to assume that the time of the injection of particles throughout the spine lasts for a similar time.

- After this time we calculate the actual γ_{cool} at the given time, and assume that the particle distribution vanishes for $\gamma > \gamma_{\text{cool}}$. We neglect adiabatic losses, for simplicity.
- We then calculate the new values of $\langle \gamma \rangle$ and $\langle \gamma^2 \rangle$ and the new value of Γ .
- We invert Eq. 1 and finally find Γ_s .

For illustration, Fig. 6 shows the evolution of the bulk Lorentz factor in the case of the parameters used for Mkn 421. We show the bulk Lorentz factor as measured by the layer and also by the observer at earth, but both as a function of the distance as measured in the frame of the layer. We also show the logarithm of γ_{cool} . As can be seen, the recoil is very significant, decelerating the spine from $\Gamma_s = 17$ to $\Gamma_s = 7.5$ within the layer. Note that $\Gamma = 3$ is the bulk Lorentz of the layer, which is therefore the minimum value which the spine could attain.

5. GeV and TeV radiogalaxies?

Also the slow layer produces a lot of GeV radiation, which remains visible even at large viewing angles (consider that $\theta = 1/\Gamma_{\text{layer}} \sim 20^\circ$). Therefore also radiogalaxies should be high energy emitters. Indeed, the three radiogalaxies detected at high energies so far, shown Fig. 7, show the characteristic double bump SED typical of blazars, suggesting a similar origin of their emission. This is more clear in Fig. 8, which compares directly the averaged SED of blazars with the SED of Cen A, NGC 6251 and M 87.

For Cen A and NGC 6251, which have been identified with EGRET sources, we measure a ratio between the EGRET (νF_ν) flux at 100 MeV and the radio flux of the core at 5 GHz which is 60 and 300, respectively.

If all FR I radiogalaxies have a similar γ -ray to radio flux ratio, we can identify the best candidates for detection in future AGILE and GLAST observations. To this aim, we will simply assume that

$$\log \nu_\gamma F_\gamma = (2 \pm 0.5) \log \nu_R F_{R,\text{core}} \quad (12)$$

where $F_{R,\text{core}}$ is the radio flux of the core at 5 GHz (Giovannini et al. 1998; Chiaberge, Capetti & Celotti 1999 and references therein), and F_γ is the γ -ray flux at 100 MeV. In Tab. 3 we list the FR I radiogalaxies belonging to the 3C sample sample, in order of decreasing nuclear radio power, and the corresponding predicted 100 MeV flux. Assuming a sensitivity limit of $\sim 5 \times 10^{-13}$ erg cm $^{-2}$ s $^{-1}$ for a relatively short exposure of GLAST, we have that more than a dozen FR I radiogalaxies can be detected.

6. Discussion

We have explored the radiative and dynamical consequences of a structured jet, in which a slow jet layer is cospatial to a fast jet spine. The motivations for this study are primarily observational, since radio data have recently found slow or null proper motion for the parsec scale radio knots in TeV emitting BL Lacs. In addition, detailed VLBI radio maps show hints of a limb brightening for the jet in Mkn 501. The main results of our study are:

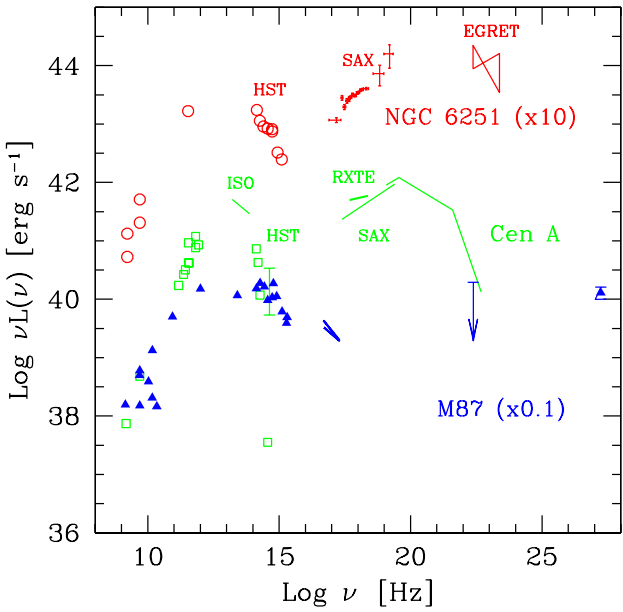


Fig. 7. The SED of NGC 6251, Cen A and M87. The data of NGC 6251 and M87, for clarity, have been vertically shifted by the labelled amount. Note that the SED of these radio galaxies show the same two-bump structure of blazars, as illustrated also in Fig. 8. Data for M87 are taken from Reimer, Protheroe & Donea (2004) and reference therein, except for the X-rays (Marshall et al. 2002), and the EGRET upper limit (Fichtel et al. 1994).

Name	$\log F_{\text{R,core}}$ (5 GHz) erg cm $^{-2}$ s $^{-1}$ Hz $^{-1}$	$\log \nu_{\gamma} F_{\gamma}$ (100 MeV) erg cm $^{-2}$ s $^{-1}$
3C 84	-21.37	-9.67 \pm 0.5
3C 274	-22.40	-10.70 \pm 0.5
3C 78	-23.02	-11.32 \pm 0.5
3C 317	-23.41	-11.71 \pm 0.5
3C 270	-23.51	-11.81 \pm 0.5
3C 465	-23.57	-11.87 \pm 0.5
3C 346	-23.66	-11.96 \pm 0.5
3C 264	-23.70	-12.00 \pm 0.5
3C 66	-23.74	-12.04 \pm 0.5
3C 272.1	-23.74	-12.05 \pm 0.5
3C 315	-23.82	-12.12 \pm 0.5
3C 338	-23.98	-12.28 \pm 0.5
3C 293	-24.00	-12.30 \pm 0.5
3C 29	-24.03	-12.33 \pm 0.5
3C 31	-24.04	-12.34 \pm 0.5
3C 310	-24.10	-12.40 \pm 0.5
3C 296	-24.11	-12.41 \pm 0.5
3C 89	-24.31	-12.61 \pm 0.5
3C 75	-24.41	-12.71 \pm 0.5
3C 449	-24.43	-12.73 \pm 0.5
3C 288	-24.52	-12.82 \pm 0.5
3C 305	-24.53	-12.83 \pm 0.5
3C 83.1	-24.68	-12.98 \pm 0.5
3C 424	-24.74	-13.05 \pm 0.5
3C 438	-24.77	-13.07 \pm 0.5
3C 386	-24.77	-13.07 \pm 0.5
3C 277.3	-24.91	-13.21 \pm 0.5
3C 348	-25.00	-13.30 \pm 0.5
3C 433	-25.30	-13.60 \pm 0.5
3C 442	-25.70	-14.00 \pm 0.5

Table 3. Radio core fluxes at 5 GHz for 3CR FR I and predicted gamma-ray fluxes.

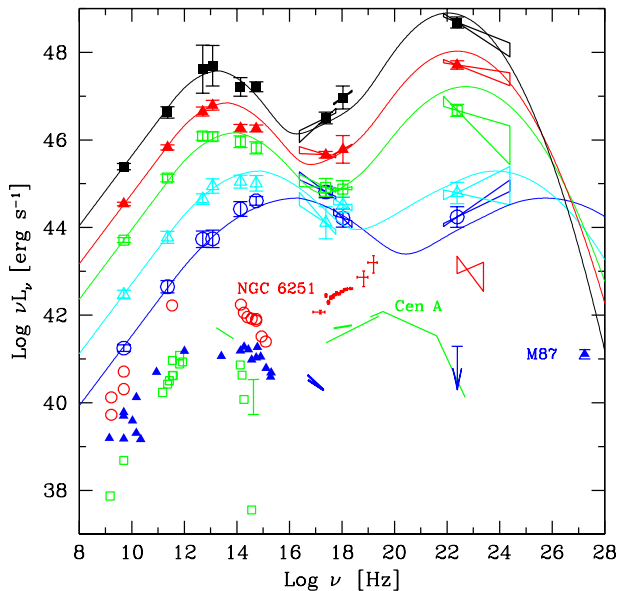


Fig. 8. The SEDs of NGC 6251, Cen A and M87 are compared with the blazar sequence, as proposed by Fossati et al. (1998). The hard X-ray [2–10 keV] spectra of blazars come from the work of Donato et al. (2001).

– The jet may be born as structured, or it may be born with equal layer/spine velocities, with the layer being decelerated in the first $\sim 10^{17}$ cm from the central black hole. As long as the layer is dissipative, our results are independent of the why there is a spine+layer structure. However, we note that the accretion disk in low power BL Lacs could be characterized by a low-efficiency accretion mode, and one of the proposed accretion disk solution in this case is the ADIOS structure (Blandford & Begelman 1999), predicting that a sizeable fraction of the accreting mass at large radii, instead to inward spiralling, leaves the disk in the form of an outflow. In this case, in the close vicinity of the black hole, the ambient medium should be relatively dense, favoring the interaction of the jet walls with the external medium. This may cause the formation of the slow layer, and at the same time this interaction may be the primary cause for the transformation of the kinetic energy of the layer into random energy and then radiation.

A low-radiative accretion disk could also explain why the broad line emission is small in BL Lac objects and in FR I radio galaxies. Further evidence of a change in the accretion mode between FR I and FR II radio galaxies is provided by the “dividing line” between these two classes of sources

in the radio-luminosity–host galaxy optical luminosity, as discussed by Ghisellini & Celotti (2001).

- If indeed the jet forms (or is born with) a layer+spine structure, then there is a radiative interplay or feedback between the two parts: each component would see an enhanced radiation field coming from the other component. This would inevitably boost the inverse Compton radiation with respect to a completely homogeneous jet.
- It is also quite clear that, for an observed Compton to synchrotron power ratio, the fact that the radiation field is enhanced also implies an increase of the magnetic field, with respect to an homogeneous source. This can solve an otherwise puzzling characteristic of HBL in general and TeV BL Lacs in particular: fitted with an homogeneous SSC model, they turn out to have very small magnetic fields, which are more under–equipartition (with the emitting particles) than in other blazars. Here we can fit the observed spectra equally well (not surprisingly, given that the free parameters are more than in the homogeneous SSC model) with equipartition magnetic fields.
- Another important consequence of having greater magnetic fields is that a smaller number of electrons can produce the observed SED. This means that the global energetic demand of the jet is reduced with respect to a homogeneous SSC model.
- The fact that the dominant inverse Compton radiation is through scattering with “external” photons implies that the emission is highly anisotropic also in the comoving frame of the spine. To conserve momentum, the emitting spine must recoil and therefore decelerate. This is a manifestation of the “Compton rocket” effect, studied in the early eighties (see e.g. O’Dell 1981) as a mean to radiatively accelerate jets. Somewhat ironically, we have shown here that this process can be important for the opposite reason. There is a precise link between TeV emission and deceleration, due to two reasons: i) TeV emitting BL Lacs have the least powerful jets, and yet they move with bulk Lorentz factor equal or greater than the ones of other blazars; ii) to produce a significant TeV radiation, the mean energy of the emitting electrons must be large. Then in these sources we have $\langle \gamma \rangle m_e \sim m_p$: the power carried by the jet in the form of protons and electrons is similar.

We then propose that the jet deceleration at small (sub–pc) scales is more efficient in low power jets emitting high energy radiation. Consider also that the initially fastest sources are the ones suffering the most severe Compton rocket effect.

- Also the inverse Compton emission from the layer is enhanced by the extra seed photons coming from the spine. This could be the reason why also radiogalaxies are relatively strong γ –ray emitters. If this is the reason, then the layer and the spine must be cospatial, and therefore the γ –ray emitting layer must be located at ~ 100 Schwarzschild radii, as the spine. The γ –ray flux observed in radiogalaxies should then be variable, with timescales of the order of $t_{\text{var}} \sim (R/c)/\delta_l \sim$ a day or less, very similar (albeit somewhat longer, due to the smaller Doppler factor) to the typical variability timescale in blazars. We propose this as

a crucial test for our scenario. Note that Cen A is already known to vary with short timescales (0.5–4 days) in the γ –ray band (Kinzer et al. 1995; Steinle et al. 1998).

- A few radiogalaxies have been already detected at high energies. The SED of their nuclear emission shows the characteristic double peak characteristic of blazars, and like these sources they can be “Compton dominated” (namely, the high energy component is more luminous than the synchrotron component). These general features are quite easily explained in the layer+spine scenario. We have then tried to predict which are the best candidate radiogalaxies to be detected by the future GLAST mission, assuming a twenty–fold increase in sensitivity with respect to EGRET. As a result, more than a dozen FR I radiogalaxies should be detectable by GLAST, if their radio to 100 MeV flux ratio is similar to the one of the three objects already identified by EGRET and by TeV Cherenkov telescopes.

References

Aharonian F., Akhperjanian A., Beilicke M. et al., 2003, A&A, 403 L1

Blandford R.D. & Begelman M.C., 1999, MNRAS, 303, L1

Bodo G., Rossi P., Mignone A., Massaglia S. & Ferrari A., 2003, NewAR, 47, 557

Cassaro P., Stanghellini C., Bondi M., Dallacasa D., Chiaberge M., Capetti A., & Celotti A., 1999, A&A, 349, 77

Chiaberge M., Celotti A., Capetti A. & Ghisellini G., 2000, A&A, 358, 104

Chiaberge M., Gilli, R., Capetti A., Macchetto F.D., 2003, ApJ, 97, 166

Chiaberge M., Capetti A. & Celotti A., 2001, MNRAS, 324, L33

Costamante L. & Ghisellini G., 2002, A&A, 384, 56

Dermer C.D., 1995, ApJ, 446, L63

Djannati-Atai A., Piron F., Barrau A. et al., A&A, 350, 17

Donato D., Ghisellini G., Tagliaferri G. & Fossati G., 2001, A&A, 375, 739

Dondi L. & Ghisellini G., 1995, MNRAS, 273, 583

Edwards P.G. & Piner B.G., 2002, ApJ, 579, L70

Ferrari A., 1998, ARA&A, 36, 539

Fichtel C.E., Bertsch D.L., Chiang J. et al., 1994, ApJS, 94, 551

Fossati G., Maraschi L., Celotti A., Comastri A. & Ghisellini G., 1998, MNRAS, 299, 433

Georganopoulos M. & Kazanas D., 2003, ApJ, 594, L27 (GK03)

Ghisellini G., 1999, Astron. Nachrichten, 320, 232.

Ghisellini G. & Celotti A., 2001, A&A, 379, L1

Ghisellini G., Celotti A., Fossati G., Maraschi L. & Comastri A., 1998, MNRAS, 301, 451

Ghisellini G., Celotti A. & Costamante L., 2002, A&A, 386, 833

Giommi P. & Padovani P., 1995, MNRAS, 277, 1477

Giovannini G., Feretti L., Gregorini L., & Parma P., 1988, A&A, 199, 73

Giovannini G., Taylor G.B., Arbizzani E. et al., 1999, ApJ, 522, 101

Giroletti M., Giovannini G., Feretti L. et al., 2004, ApJ, 600, 127

Guetta D., Ghisellini G., Lazzati D. & Celotti A., 2004, A&A in press (astro-ph/0402164)

Hartman R.C., Bertsch S.D., Bloom S.D. et al., 1999, ApJS, 123, 79

Henri, G. & Pelletier, G. 1991, ApJ, 383, L7

Katarzynski K., Sol H. & Kus A., 2003, A&A, 410, 101

Kino M., Takahara F. & Kusunose M., 2002, ApJ, 564, 97

Kinzer R.L., Johnson W.N., Dermer C.D. et al., ApJ, 449, 105

Komissarov S.S., 1990, *SvA Letters*, 16, 284

Konopelko K., Mastichiadis A., Kirk J., De Jager O.C. & Stecker F.W., 2003, *ApJ*, 597, 851

Krawczynski H., Coppi P.S. & Aharonian F., 2002, *MNRAS*, 336, 721

Krawczynski H., Hughes S.B., Horan, D. et al., 2004, *ApJ*, 601, 151

Laing R.A., 1993, in: *Astrophysical jets*, Space Telescope Sci. Inst. Symp. 6, eds: Burgarella D., Livio M. & O'Dea C.P., Cambridge Univ. Press, p. 95

Laing R.A., Riley J.M. & Longair M.S., 1983, *MNRAS*, 204, 151

Morganti R., Fosbury R.A.E., Hook R.N., Robinson A. & Tsvetanov Z. 1992, *MNRAS*, 256, P1

Marshall H.L., Miller B.P., Davis D.S., Perlman E.S., Wise M., Canizares C.R. & Harris D.E. 2002, *ApJ*, 564, 683

Mukherjee R., Halpern J., Mirabal N. & Gotthelf E.V., 2002, *ApJ*, 574, 693

O'Dell S.L., 1981, *ApJ*, 243, L147

Owen F.N., Hardee P.E. & Cornwell T.J., 1989, *ApJ* 340, 698

Pian E., Vacanti G., Tagliaferri G. et al., 1998, *ApJ*, 492, L17

Piner B.G. & Edwards P.G., 2004, *ApJ*, 600, 115

Rawlings S.G. & Saunders R.D.E., 1991, *Nature*, 349, 138

Reimer A., Protheroe R.J. & Donea A.-C., 2004, *A&A* 419, 89

Rybicki G.B. & Lightman A.P., 1979, *Radiative Processes in Astrophysics*, New Youk, Wiley Interscience

Rossi E.M., Lazzati D. & Rees, M.J., 2002, *MNRAS*. 332, 945

Sikora M., Sol H., Begelman M.C. & Madejski G.M., 1996, *MNRAS*, 280, 781

Spada M., Ghisellini G., Lazzati D & Celotti A., 2001, *MNRAS*, 325, 1559

Stawarz L. Sikora M., Ostrowski M. & Begelman M.C., 2004, *ApJ*, in press (astro-ph/0401356)

Steinle H., Bennet K., Bloemen H. et al., 1998, *A&A*, 330, 97

Swain M.R., Bridle A.H. & Baum S.A., 1998, *ApJ*, 507, L29

Tavecchio F., Maraschi L. & Ghisellini G., 1998. *ApJ*, 509, 608

Tavecchio F., Maraschi L., Pian E. et al., 2001, *ApJ*, 554, 725

Zhang B. & Meszaros P., 2002, *ApJ*, 571, 876